IEEE Access
Multidisciplinary | Rapid Review | Open Access Journal

Received June 25, 2019, accepted July 6, 2019, date of publication July 15, 2019, date of current version August 6, 2019.

Digital Object Identifier 10.1109/ACCESS.2019.2928856

Double Closed-Loop Controller Design for Boost Pressure Control of Turbocharged Gasoline Engines

XUN GONG[1,2,3], YAOHAN WANG[2], HUAN CHEN[2], AND YUNFENG HU[1,2]

[1]State Key Laboratory of Automotive Simulation and Control, Jilin University, Changchun 130022, China
[2]Department of Control Science and Engineering, Jilin University, Changchun 130022, China
[3]Department of Artificial Intelligence, Jilin University, Changchun 130022, China

Corresponding author: Yunfeng Hu (huyf@jlu.edu.cn)

This work was supported in part by the National Natural Science Foundation of China under Grant 61703177, Grant U1864201, and Grant 61773009, in part by the Jilin Provincial Science Foundation of China under Grant 20190302119GX and Grant 20180101037JC, in part by the Jilin Provincial Development and Reform Commission Foundation of China under Grant 2019C036-4, and in part by the Funds for the Joint Project of Jilin Province and Jilin University under Grant SXGJSF2017-2-1-1.

ABSTRACT The precise boost pressure control is the key to guaranteeing reliable turbocharged gasoline engine operation. The closed-loop control requires fast boost pressure tracking performance in wide engine operating range. This paper presents a double closed-loop nonlinear control scheme to improve transient tracking performance. The air-path system of the turbocharged gasoline engine is described by a physics-based, nonlinear, mean value model that presents a long regulation channel from the control input, wastegate-opening, to the control output, boost pressure and brings challenges for the controller design with satisfied tracking performance. To address this problem, the outer loop treats the turbine speed as a downstream control demand and adjusts it by using a feedforward-feedback control to achieve fast boost pressure tracking. Subsequently, a disturbance-observer-based nonlinear inner-loop controller is designed to regulate the wastegate that stabilizes the turbine speed tracking error while handles the uncertainties due to operating variation. The stability of the whole closed-loop system is analyzed by the Lyapunov stability theory and the robustness against operating variation is discussed based on input to state stability (ISS). The effectiveness of the proposed controller is validated through a higher fidelity model in AMESim and its performances are compared with well-tuned baseline controllers.

INDEX TERMS Turbocharged gasoline engine, boost pressure, double closed-loop control, stability and robustness.

I. INTRODUCTION

Nowadays, the turbocharger is widely adopted to enable the downsize of gasoline engines where a compressor is used to increase the density of the intake air, thereby boost the engine power to meet the driver demand with higher fuel efficiency [1]–[3]. The advantages of boosting are accompanied by an increase in complexity of the air-path control system design and it is essential to develop a reliable control strategy to achieve good performance.

As the torque-based control scheme suggests, the desired torque of a turbocharged gasoline engine can be calculated from the driver pedal position and then mapped into the desired intake manifold pressure and boost pressure considering fuel economy and emission [4]. These two desired pressure targets are then tracked by regulating the throttle and wastegate [5], [6]. Given the complexity of the turbo-charged engine system and multiple control requirements, Model Predictive Control (MPC) approaches [7]–[9] are effective with meaningful objective functions to coordinately regulate the multiple actuators [10]–[12]. Considering the complex nonlinear empirical engine air-path models, researchers are turning to learning-based MPC design [13]. Since implementing MPC in coordinated engine control requires meeting strict real-time requirements in terms of execution speed and memory allocation, decentralized control scheme is an alternative solution in practice where the multiple pressures tracking problem can be handled with independent

The associate editor coordinating the review of this manuscript and approving it for publication was Ning Sun.

controllers, e.g. regulating the throttle to track the desired intake manifold pressure, and regulating the wastegate to track the desired boost-pressure [14]. A motion planning feedforward control combined with a gain scheduled feedback control was designed to track the desired boost pressure in [15]. To handle the nonlinearity of the air-path system, an adaptive internal model control scheme based on structured quasi-linear parameter-varying model was applied to control the boost pressure in [16], [17] and [18]. In [14], a gain scheduled controller was proposed to track the desired intake manifold pressure and boost pressure. To account for the influence of time-delay, modeling uncertainties and the bounded disturbance, a robust H_∞ controller based on a switching Takagi-Sugeno (TS) model was designed [19]. In [20], a fuzzy controller based on the switching TS fuzzy model was developed to regulate the throttle and wastegate. The existing control methods mainly focused on adopting the single closed-loop control scheme. Typically, the turbocharged engine system is a high-order nonlinear system with a long input-output regulation channel where the nonlinearity, large inertia, and uncertainties should be handled. The single closed-loop control scheme may limit the control performance and space still exists to improve the transient control performance.

Motivated by the successful applications in advanced automotive powertrain systems [21], [22], this paper explores the double closed-loop nonlinear control scheme for a turbocharged gasoline engine driven by the need for robust boost pressure tracking control in wide-range operating conditions. To this end, we mainly focus on the tracking control of the boost pressure, and assume that the manifold pressure is well controlled by the throttle. The proposed double closed-loop controller includes an outer-loop feedfoward-feedback controller that tracks the boost pressure set-points and generates the turbine speed demand, and an inner-loop disturbance-observer-based nonlinear controller that stabilizes the turbine speed tracking error. The stability and robustness of the whole control system is theoretically guaranteed and the control performance is validated through a higher fidelity turbo-charged engine in simulation. The main contributions of this paper are threefold as follows.

(i) To facilitate the nonlinear controller design, the dynamics of the air-path system of a turbocharged gasoline engine is described by a third-order, control-oriented, mean value model;

(ii) Considering the long regulation channel in turbocharged gasoline engines, a double closed-loop control scheme is developed for the boost pressure tracking problem. To achieve fast boost pressure tracking, an outer-loop controller is designed that includes a neural-network-based feedforward control and a PID feedback control where the turbine speed is treated as a virtual control input. To stabilize the turbine speed tracking error and handle uncertainties, a disturbance observer-based inner loop controller is deduced by using Backstepping technique;

(iii) The stability and robustness of the whole closed-loop system are discussed theoretically by the Lyapunov stability theory and ISS theories.

The rest of this paper is organized as follows. In Section II, the control problem is stated and the control-oriented, nonlinear mean value model of a turbocharged gasoline engine is described. Section III proposes the double closed-loop control scheme and analyzes the closed-loop stability and robustness. Section IV presents the simulation results. Section V summaries the key findings of this paper.

II. PROBLEM STATEMENT AND CONTROL-ORIENTED MODEL

In this paper, a four cylinder, turbocharged, gasoline engine is considered and the schematics of the system is shown in Fig. 1. The engine intake port is connected to the compressor where the fresh air is boosted to a higher density level and passes through the throttle before entering the engine intake manifold and the cylinder. The engine exhaust port is connected to the turbine that is mechanically connected to the compressor. The electronic wastegate valve is the key actuator that regulates the opening of the turbine bypass, affecting the turbine speed and therefore the boost pressure.

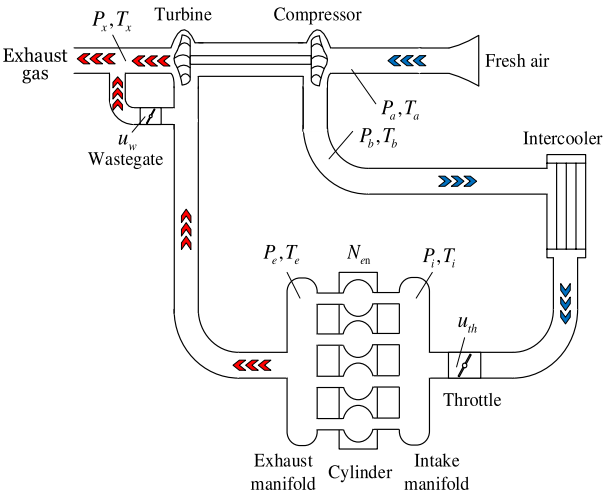

FIGURE 1. Schematic diagram of a turbocharged gasoline engine.

A. CONTROL PROBLEM STATEMENT

The control objective is to make the turbocharged gasoline engine track a desired boost pressure reference P_b^* via the regulation of the wastegate. Note that good tracking of the boost pressure will ensure that the throttle is fully open in the turbocharging operating zone [23]. In this paper, we will only focus on using the wastegate to track the boost pressure while the throttle is considered as an exogenous input. Measurements for boost pressure, P_b, temperature variables, T_b, T_i, T_x, compressor/turbine speed, N_t, engine speed, N_{en}, throttle opening angle, u_{th}, are assumed to be available for feedfoward and feedback control. To proceed the nonlinear

controller design, the control-oriented model of the turbocharged gasoline engine are introduced as below.

B. CONTROL-ORIENTED MODEL

In this paper, the nonlinear control-oriented model for the boost pressure control follows the mean value aspect and includes several subsystems described as follows.

Boosted air dynamics: This model describes the air-flow dynamics that the fresh air is compressed into the engine. In this process, the compressor is driven by the exhaust air-flow via the turbine. According to the mass flow balance equation and the ideal gas law, the dynamics of the boost pressure P_b is given by [24], [25]

$$\frac{dP_b}{dt} = \frac{RT_b}{V_b}(W_c - W_{th}), \tag{1}$$

where R is the ideal gas constant, T_b is the temperature of air at the compressor outlet, V_b is the volume of compressor, W_c is the compressor air mass flow rate, W_{th} is throttle air mass flow rate.

As described in [26], [27], the compressor mass flow rate can be modeled by

$$W_c = \frac{P_a}{P_{st}}\sqrt{\frac{T_{st}}{T_a}} f_c(P_b, N_{t,cor}), \tag{2}$$

where P_a is the ambient pressure, P_{st} is the standard pressure, T_a is the ambient temperature, T_{st} is the standard temperature, and $f_c(\cdot)$ is the corrected compressor air mass flow rate presented by a polynomial equation as

$$f_c(P_b, N_{t,cor}) = \alpha_1 + \alpha_2 N_{t,cor} + \alpha_3 P_b + \alpha_4 N_{t,cor}^2 + \alpha_5 N_{t,cor} P_b + \alpha_6 P_b^2, \tag{3}$$

where $\alpha_1 = 0.46, \alpha_2 = -2.71 \times 10^{-6}, \alpha_3 = -2.71 \times 10^{-6}, \alpha_4 = 4.98 \times 10^{-6}, \alpha_5 = 3.82 \times 10^{-6}, \alpha_6 = -1.57 \times 10^{-6}$ are fitting parameters, $N_{t,cor} = \sqrt{\frac{T_{st}}{T_a}} N_t$ is the corrected turbine rotational speed, N_t is the turbine rotational speed.

Turbine air mass flow: The mass flow rate through turbine is presented by

$$W_t = f_t\left(\frac{P_e}{P_x}, \frac{N_t}{\sqrt{T_e}}\right)\frac{P_e}{\sqrt{T_e}}, \tag{4}$$

where P_x is the outlet pressure of turbine, P_e is the exhaust manifold pressure, T_e is the exhaust manifold temperature, $f_t(\cdot)$ is the corrected mass flow rate of turbine and calculated by a specific look-up table.

Throttle air mass flow: The air mass flow through throttle is modeled based on the standard equations of compressible gas flow through a nozzle [3] as

$$W_{th} = \frac{f_{th}(sat(0, u_{th}, 100))}{\sqrt{T_b}} C_q P_b \phi(\Pi_t), \tag{5}$$

where u_{th} is the throttle opening angle considered as an exogenous input, and $f_{th}(\cdot)$ denotes the orifice opening area characterized by a look-up table with a saturation function $sat(\cdot)$ that limits throttle opening within the range [0,100], C_q is the air discharge coefficient, and $\phi(\Pi_t)$ is the mass flow function defined by

$$\phi(\Pi_t) = \begin{cases} \sqrt{\frac{2\gamma}{R(\gamma-1)}\left[(\Pi_t)^{\frac{2}{\gamma}} - (\Pi_t)^{\frac{\gamma+1}{\gamma}}\right]}, \\ \qquad \Pi_t > \left(\frac{2}{\gamma+1}\right)^{\frac{\gamma-1}{\gamma}} \\ \sqrt{\frac{\gamma}{R}\left(\frac{2}{\gamma+1}\right)^{\frac{\gamma+1}{\gamma-1}}}, \\ \qquad \Pi_t \le \left(\frac{2}{\gamma+1}\right)^{\frac{\gamma-1}{\gamma}} \end{cases} \tag{6}$$

where γ is the specific heat ratio, P_i is the intake manifold pressure, and $\Pi_t = \frac{P_i}{P_b}$ denotes the intake pressure ratio.

Cylinder air mass flow: The engine cylinder is considered as a volumetric pump, i.e. a device that enforces a volume flow approximately proportional to its speed

$$W_{en} = \frac{\eta_{en} V_{en}}{120 R T_i} N_{en} P_i, \tag{7}$$

where V_{en} is the total volume of four cylinders, η_{en} is the volumetric efficiency characterized by a look-up table, T_i is the intake manifold temperature, N_{en} is the engine speed which is measurable and considered as an exogenous input in this work.

Exhaust manifold air dynamics: The exhaust manifold represents the chamber between the cylinder outlet port and the turbine. The dynamics of exhaust manifold pressure is presented by

$$\frac{dP_e}{dt} = \frac{RT_e}{V_e}(W_{exh} - W_t - W_w), \tag{8}$$

where V_e is the volume of the exhaust manifold, W_t is the mass flow rate through the turbine, W_w is the air mass flow rate through the wastegate, W_{exh} is the exhaust mass flow rate computed by

$$W_{exh} = W_{en}\frac{1 + A/F}{A/F}, \tag{9}$$

where A/F is the stoichiometric air-fuel ratio of gasoline engines.

Wastegate air mass flow: The wastegate is the key actuator that adjusts the amount of exhaust gas through the turbine. Similar with the throttle, the air-flow rate through the wastegate is given by

$$W_w = \frac{f_w(sat(0, u_w, 100))}{\sqrt{T_e}} C_{qt} P_e \phi(\Pi_w), \tag{10}$$

where $sat(\cdot)$ limits u_w within the range [0, 100], $f_w(\cdot)$ is the orifice opening area calculated by

$$f_w(u_w) = (500 - 5u_w) \times 10^{-6}, \tag{11}$$

C_{qt} is the exhaust gas discharge coefficient, $\phi(\Pi_t)$ is the mass flow function for the exhaust gas defined by

$$\phi(\Pi_w)=\begin{cases}\sqrt{\dfrac{2\gamma_e}{R(\gamma_e-1)}\left[(\Pi_w)^{\frac{2}{\gamma_e}}-(\Pi_w)^{\frac{\gamma_e+1}{\gamma_e}}\right]}, \\ \qquad \Pi_w > \left(\dfrac{2}{\gamma_e+1}\right)^{\frac{\gamma_e-1}{\gamma_e}}, \\ \sqrt{\dfrac{\gamma_e}{R}\left(\dfrac{2}{\gamma_e+1}\right)^{\frac{\gamma_e+1}{\gamma_e-1}}}, \\ \qquad \Pi_w \le \left(\dfrac{2}{\gamma_e+1}\right)^{\frac{\gamma_e-1}{\gamma_e}}, \end{cases} \tag{12}$$

where γ_e is the specific heat ratio of the exhaust gas, and $\Pi_w = \frac{P_x}{P_e}$ denotes the exhaust pressure ratio.

Turbine speed dynamics: The dynamics of the rotational speed of turbine shaft N_t is modeled according to the Newton's Second law as

$$\frac{dN_t}{dt} = \frac{1}{I_t N_t}(H_t - H_c), \tag{13}$$

where H_t denotes the power generated by the turbine and H_c denotes the power consumed by the compressor, I_t represents the moment of inertia. According to the first law of thermodynamics, the power of compressor H_c can be described as

$$H_c = c_{p,a} T_a W_c \frac{1}{\eta_c}\psi_c, \tag{14}$$

where $c_{p,a}$ is the specific heat constant of the air, η_c is the isentropic efficiency of compressor characterized by a look-up table, ψ_c is the air mass flow coefficient calculated by

$$\psi_c = \left(\frac{P_b}{P_a}\right)^{\frac{\gamma-1}{\gamma}} - 1. \tag{15}$$

The power of turbine is described as

$$H_t = c_{p,e} T_e W_t \eta_t \psi_t, \tag{16}$$

where $c_{p,e}$ is the specific heat constant of the exhaust gas, η_t is the isentropic efficiency of turbine characterized by a look-up table, ψ_t is the exhaust gas mass flow coefficient calculated by

$$\psi_t = 1 - \left(\frac{P_x}{P_e}\right)^{\frac{\gamma_e-1}{\gamma_e}}. \tag{17}$$

Summarizing (1)−(17) leads to the 3rd-order control-oriented model as in (18), shown at the bottom of the next page. The structural diagram of the model is shown in Fig. 2 that illustrates the signal flow from the control input, u_w, exogenous inputs, u_{th} and N_{en}, to the output, N_{en}.

III. DOUBLE CLOSED-LOOP CONTROLLER DESIGN

A. CONTROL SYSTEM ARCHITECTURE OVERVIEW

The operating conditions vary widely in the application of turbocharged gasoline engine control. As shown in Fig. 2, since the regulation tunnel from the wastegate actuator

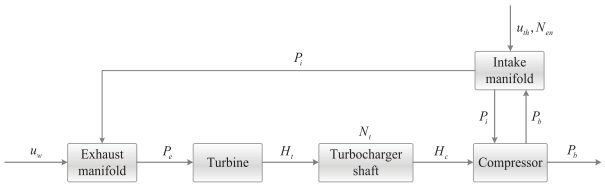

FIGURE 2. Structural diagram of the nonlinear control-oriented model.

command u_w to the boost pressure P_b is long, the variation of the exogenous signal, i.e, engine speed, N_{en}, may result in either inadequate boost at low loads or over-boost situation at high loads. The nonlinearity of (18) also adds complexity to the controller design. Double closed-loop control scheme with nonlinear feedback is adopted accounting for its advantages of good tracking performance and robustness. The schematic of the proposed double closed-loop controller is shown in Fig. 3. In the outer-loop, a Neural Network (NN)-based feedforward control combined with a Proportional-Integral-Derivative (PID) feedback control is adopted to achieve fast boost pressure tracking and calculate the virtual turbine speed control demand N_t^*. In the inner-loop, taking advantage of the strict feedback form of (18b) and (18c), a nonlinear feedback controller is derived based on Backstepping technique to stabilize the turbine speed tracking error and reject disturbance due to operating variation. The details of the controller design and the stability analysis are discussed as below.

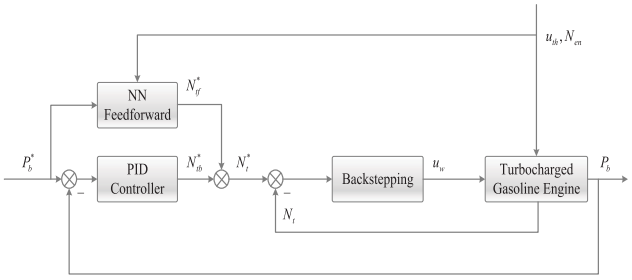

FIGURE 3. Schematic of the double closed-loop controller for boost pressure tracking.

B. OUTER-LOOP CONTROLLER DESIGN

The objective of the outer-loop controller is to design a virtual control input N_t^* (turbine speed) to make the actual boost pressure P_b tracks the given set-points P_b^*. In this paper, to obtain a fast tracking performance, the outer-loop controller is designed as

$$N_t^* = N_{tf}^* + N_{tb}^*, \tag{19}$$

where N_{tf}^* is the feedforward control and N_{tb}^* is the feedback control to be determined.

1) FEEDFORWARD CONTROL BASED ON NEURAL NETWORK

Due to the nonlinearity of the subsystem (18a) and (18b), it is not easy to explicitly obtain the feedforward control

law. In recent work on the dynamics approximation of engine air-path system [13], the neural network has proven effective in terms of both accuracy and ease of use. Therefore, in this paper, a 3-layer NN is used to learn the inversed dynamics of the subsystem (18a) and (18b) and calculate the feedforward control N_{tf}^*. The input vector of the NN is selected as $I_{NN} = [\dot{P}_b^*, P_b^*, N_{en}, u_{th}]^T$ and the output is the feedforward control law N_{tf}^*. There are 30 neurons in the hidden layer. The structure of the neural network is shown in Fig. 4.

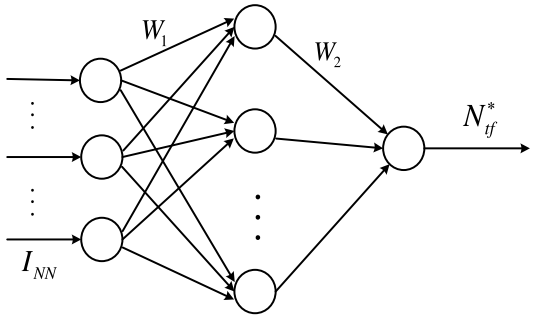

FIGURE 4. The structure of the NN-based feedforward control.

Thus, the feedforward control law is described by,

$$N_{tf}^* = W_2\phi(W_1 I_{NN} + b_1) + b_2, \tag{20}$$

where W_1 and W_2 are the weighting matrices, b_1 and b_2 are the bias vectors, $\phi(\cdot)$ represents the nonlinear activation function which is selected as the sigmoid function in this paper. All the parameters associated with the neural network are learned off-line.

2) FEEDBACK CONTROL

Define tracking error of the boost pressure as

$$e_p = P_b^* - P_b. \tag{21}$$

Considering the ideal case, if the NN-based feedforward law (20) is perfectly learned, $P_b = P_b^*$ holds and the corresponding boost pressure tracking error dynamics after applying the feedforward law yields

$$\dot{e}_p = f(P_b^*, N_{tf}^*) = 0. \tag{22}$$

However, due to learning errors of NN and external disturbances, $P_b \neq P_b^*$ by applying feedforward control thereby a feedback law N_{tb}^* is needed to compensate the tracking error. Differentiating (21) and combining (18a) leads to

$$\begin{aligned}\dot{e}_p &= \dot{P}_b^* - \dot{P}_b = f(P_b, N_t)\\ &= \dot{P}_b^* - a_1 - a_2 N_t - a_3 P_b - a_4 N_t^2 - a_5 N_t P_b\\ &\quad - a_6 P_b^2 - a_7 f_{th}(sat(0, u_{th}, 100))\phi(\Pi_t) P_b.\end{aligned} \tag{23}$$

The first order Taylor series expansion is used along (P_b^*, N_{tf}^*) to approximate (23), yielding:

$$\dot{e}_p = f(P_b^*, N_{tf}^*) + \left.\frac{\partial f}{\partial P_b}\right|_{P_b^*, N_{tf}^*} \cdot e_p + \left.\frac{\partial f}{\partial N_t}\right|_{P_b^*, N_{tf}^*} \cdot N_{tb}^* + d_1. \tag{24}$$

where the disturbance d_1 sums up the uncertainties and the residual from the Taylor series expansion. A PID controller is applied as the feedback control to stabilize the system (24),

$$N_{tb}^* = K_p e_p + K_i \int e_p dt + K_d \dot{e}_p, \tag{25}$$

where K_p, K_i and K_d are tuning parameters of the PID controller.

According to Routh-Hurwitz Stability criterion [28], we choose $K_p > 0, K_i > 0$ and $K_d > 0$ in the closed-loop system of (24) to impose

$$1 + MK_d > 0, \tag{26a}$$

$$a_3 + a_5 N_{tf}^* + 2a_6 P_b^* + a_7 f_{th} + MK_p > 0, \tag{26b}$$

$$MK_i > 0, \tag{26c}$$

where $M = a_2 + 2a_4 N_{tf}^* + a_5 P_b^*$. The closed-loop system of (24) is asymptotically stable if $d_1 == 0$ and ISS if $d_1 \neq 0$ is bounded [29]. Therefore, there exists a Lyapunov function V_o for functions $\alpha(\cdot)$, $\gamma(\cdot)$ which are belong to class $\mathcal{K}_\infty$, yielding

$$\dot{V}_o \leq -\alpha(|e_p|) + \gamma(|d_1|), \quad \forall e_p,\ d_1. \tag{27}$$

Combining the feedfword controller N_{tf}^* and feedback controller N_{tb}^* leads to the outer-loop controller which is the reference value N_t^* for the inner-loop controller.

C. INNER-LOOP CONTROLLER DESIGN

For the inner-loop controller design, we define $\bar{u}_w = f_w(sat(0, u_w, 100))$ as an intermediate control input and the actual control input u_w can be calculated explicitly by the reverse solution. The state variables are defined as $x_1 = N_t$ and $x_2 = P_e$. Thus, the state space formulation of model (18b) and (18c) is rewritten as:

$$\dot{x}_1 = f_1(P_b, x_1) + Ax_2 + f_0(x_1, x_2), \tag{28a}$$

$$\frac{dP_b}{dt} = a_1 + a_2 N_t + a_3 P_b + a_4 N_t^2 + a_5 N_t P_b + a_6 P_b^2 + a_7 f_{th}(sat(0, u_{th}, 100))\phi(\Pi_t) P_b, \tag{18a}$$

$$\frac{dN_t}{dt} = b_1\left[1 - \left(\frac{P_x}{P_e}\right)^{b_2}\right]\eta_t f_t\left(\frac{P_e}{P_x}, \frac{N_t}{\sqrt{T_e}}\right)\frac{P_e}{N_t} + b_3\frac{1}{\eta_c}\left[\left(\frac{P_b}{P_{atm}}\right)^{b_4} - 1\right] f_c(P_b, N_{t,cor})\frac{1}{N_t}, \tag{18b}$$

$$\frac{dP_e}{dt} = c_1\eta_{en} N n_{en} P n n_i + c_2 f_t\left(\frac{P_e}{P_x}, \frac{N_t}{\sqrt{T_e}}\right) P_e + c_3\phi(\Pi_w) P_e f_w(sat(0, u_w, 100)). \tag{18c}$$

$$\dot{x}_2 = f_2(x_1, x_2) + g(x_2)\bar{u}_w, \tag{28b}$$

where

$$\begin{aligned}
f_1(P_b, x_1) &= b_3 \frac{1}{\eta_c}\left[\left(\frac{P_b}{P_{atm}}\right)^{b_4} - 1\right] f_c(P_b, N_{t,cor})\frac{1}{x_1},\\
f_0(x_1, x_2) &= b_1\left[1 - \left(\frac{P_x}{P_e}\right)^{b_2}\right]\eta_t f_t\left(\frac{x_2}{P_x}, \frac{x_1}{\sqrt{T_e}}\right)\frac{x_2}{x_1} - Ax_2,\\
f_2(x_1, x_2) &= c_1\eta_{en}Nnnn_{en}Pnn_i + c_2 f_t\left(\frac{x_2}{P_x}, \frac{x_1}{\sqrt{T_e}}\right)x_2,\\
g(x_2) &= c_3\phi(\Pi_w)x_2,
\end{aligned} \tag{29}$$

and $A \neq 0$ is a constant.

Due to the high nonlinearity of $f_0(x_1, x_2)$, it is treated as a modeling uncertainty and a linear extended state observer (ESO) [30], [31] is applied to estimate its value. To this end, we define $z_1 = x_1$ and an extended state $z_2 = f_0(x_1, x_2)$. Then, (28a) is extended to

$$\begin{aligned}
\dot{z}_1 &= f_1(P_b, z_1) + Ax_2 + z_2,\\
\dot{z}_2 &= h(t),
\end{aligned} \tag{30}$$

where $h(t)$ is considered as an unknown term with respect to the time instant t.

Then, we define the estimated error $\tilde{z}_1 = z_1 - \hat{z}_1$ and the linear ESO is described by

$$\begin{aligned}
\dot{\hat{z}}_1 &= f_1(P_b, \hat{z}_1) + Ax_2 + \hat{z}_2 + 2\lambda_o\tilde{z}_1,\\
\dot{\hat{z}}_2 &= \lambda_o^2\tilde{z}_1,
\end{aligned} \tag{31}$$

where $[2\lambda_o\ \lambda_o^2]$ is the vector of the observer gains as suggested in [32] and λ_o is tuned according to the convergence time. Hence, $f_0(x_1, x_2)$ is estimated by

$$\hat{f}_0(x_1, x_2) = \hat{z}_2. \tag{32}$$

Combining (28) with ESO (31), the state space equation of the inner-loop system is written as

$$\dot{x}_1 = f_1(P_b, x_1) + Ax_2 + \hat{z}_2 + d_2, \tag{33a}$$

$$\dot{x}_2 = f_2(x_1, x_2) + g(x_2)\bar{u}_w + d_3, \tag{33b}$$

where disturbances d_2 and d_3 sum up the uncertainties due to the observed error of ESO and the operating variation of the engine system.

The control objective for the inner-loop system is to track the desired reference of turbine speed N_t^* obtained by the outer-loop controller. The second-order inner-loop system (33) appears to be a strict feedback formulation to which the Backstepping technique [33] is suitable for the closed-loop controller design as the design process is intuitive and the robust stability can be guaranteed based on Lyapunov and ISS theories. We define the tracking error as $e_1 = N_t^* - x_1$. The state x_2 can be viewed as a virtual control input for (33a) and a Lyapunov function is selected accordingly as:

$$V_1 = \frac{1}{2}en_1^2 + \frac{k_1}{2}\chi^2, \tag{34}$$

where $\chi = \int e_1\, dt$ and $k_1 > 0$.

Differentiating (34) with respect to time, yields

$$\begin{aligned}
\dot{V}_1 &= e_1\dot{e}_1 + k_1\chi e_1\\
&= e_1[\dot{N}_t^* - f_1(P_b, x_1) - Ax_2 - \hat{z}_2 + k_1\chi - d_2]\\
&\leq e_1[\dot{N}_t^* - f_1(P_b, x_1) - Ax_2 - \hat{z}_2 + k_1\chi] + \frac{e_1^2}{2} + \frac{d_2^2}{2}\\
&= e_1[\dot{N}_t^* - f_1(P_b, x_1) - Ax_2 - \hat{z}_2 + \frac{e_1}{2} + k_1\chi] + \frac{d_2^2}{2}.
\end{aligned} \tag{35}$$

Choose the virtual control input as

$$x_{2d} = \frac{1}{A}[k_2e_1 + \dot{N}_t^* - f_1(P_b, x_1) - \hat{z}_2 + \frac{e_1}{2} + k_1\chi], \tag{36}$$

to impose that

$$\dot{V}_1 \leq -k_2e_1^2 + \frac{d_2^2}{2}, \tag{37}$$

where $k_2 > 0$. If the disturbance $d_2 = 0$, (37) is non-positive as $\dot{V}_1 < 0$ ($e_1 = 0 \Leftrightarrow \dot{V}_1 = 0$), so that the closed-loop system of (33a) is asymptotically stable. If the disturbance $d_2 \neq 0$ is bounded, the system (33a) is ISS.

In (33b), to ensure that x_2 asymptotically converges to x_{2d}, we define an additional error state as

$$e_2 = x_{2d} - x_2. \tag{38}$$

Differentiating (38) leads to

$$\dot{e}_2 = \dot{x}_{2d} - \dot{x}_2 = \dot{x}_{2d} - f_2(x_1, x_2) - g(x_2)\bar{u}_w - d_3, \tag{39}$$

Then, the Lyapunov function (34) is extended to

$$V_2 = V_1 + \frac{1}{2}ennn_2^2. \tag{40}$$

Differentiate (40) with respect to time leads to

$$\begin{aligned}
\dot{V}_2 &= e_1\dot{e}_1 + k_1\chi e_1 + e_2\dot{e}_2\\
&= e_1[N_t^* - f_1(P_b, x_1) - Ax_2 - \hat{z}_2 + k_1\chi - d_2]\\
&\quad + e_2[\dot{x}_{2d} - f_2(x_1, x_2) - g(x_2)\bar{u}_w - d_3]\\
&\leq e_1[N_t^* - f_1(P_b, x_1) - Ax_{2d} - \hat{z}_2 + \frac{e_1}{2} + k_1\chi]\\
&\quad + e_2[\dot{x}_{2d} - f_2(x_1, x_2) - g(x_2)\bar{u}_w + Ae_1 + \frac{e_2}{2}] + \frac{d_2^2 + d_1^2}{2}\\
&= -k_1e_1^2 + e_2[\dot{x}_{2d} - f_2(x_1, x_2) - g(x_2)\bar{u}_w + Ae_1 + \frac{e_2}{2}]\\
&\quad + \frac{d_2^2 + d_3^2}{2},
\end{aligned} \tag{41}$$

where $g(x_2) \neq 0$ in normal operating condition of turbo-charged in practice.

Thus, we choose the control input as

$$\bar{u}_w = \frac{1}{g(x_2)}[k_3e_2 + \dot{x}_{2d} - f_2(x_1, x_2) + Ae_1 + \frac{e_2}{2}], \tag{42}$$

with $k_3 > 0$ that guarantees

$$\dot{V}_2 = -k_2e_1^2 - k_3e_2^2 + \frac{d_2^2 + d_3^2}{2}. \tag{43}$$

For (43), if $\frac{d_2^2+d_3^2}{2} = 0$, the above inequality is changed as $\dot{V}_2 \leq 0$ ($e_1 = 0$, $e_2 = 0 \Leftrightarrow \dot{V}_2 = 0$), then the closed error system (33b) is asymptotically stable; If $\frac{d_2^2+d_3^2}{2} \neq 0$ is bounded, the system is ISS and robust against d_2 and d_3.

Finally, according to (11), the actual command of the wastegate actuator can be calculated.

D. STABILITY ANALYSIS OF THE WHOLE CLOSED-LOOP SYSTEM

The Lyapunov function of the whole closed-loop system is given by

$$V_t = V_0 + V_2. \tag{44}$$

Differentiating (44) and combining (27) and (43) leads to

$$\begin{aligned}\dot{V}_t &= \dot{V}_0 + \dot{V}_2 \\ &\leq -\alpha(|e_p|) - k_2 e_1^2 - k_3 e_2^2 + \gamma(|d_1|) + \frac{d_2^2 + d_3^2}{2}.\end{aligned} \tag{45}$$

Therefore, the total closed-loop system is asymptotically stable if $\gamma(|d_1|) + \frac{d_2^2+d_3^2}{2} = 0$, and ISS if the bounded disturbance $\gamma(|d_1|) + \frac{d_2^2+d_3^2}{2} \neq 0$.

IV. SIMULATION RESULTS AND DISCUSSION

To evaluate the performance of the proposed double closed-loop control scheme, a higher fidelity simulation model of the turbocharged gasoline engine is developed in the simulation environment of the commercial software LMS Imagine.Lab AMESim (Rev 13). The internal combustion engine model in AMESim is selected as CFM 1D model from IFP-Engine library which includes the detailed mechanical parts of the engine and is able to capture most of significant dynamics of turbocharged gasoline engines. The layout of the higher fidelity model is shown in Fig. 5. The tuning parameters of the proposed controller are given as follows: 1) Outer-loop feedback controller: $K_p = 0.6$, $K_i = 0.1$, $K_d = 0.0001$; 2) Inner-loop Backstepping controller: $k_1 = 0.3$, $k_2 = 15$, $k_3 = 12$.

A. PERFORMANCE EVALUATION ON TRANSIENT TRACKING CONTROL

The following control specifications are considered [18]: (1)

(i) The overshoot of P_b while tracking a step change reference should be as small as possible;

(ii) The oscillation of P_b while tracking a step change reference should be avoided as the corresponding torque oscillation is noticeable to the driver.

The transient tracking performance is shown in Fig. 6 and Fig. 7. In simulation, the nominal engine speed is set as 3000 *rpm* and the desired boost pressure is set as a step-changed signal while the throttle position is set as fully open. In Fig. 6, the proposed double closed-loop controller achieves fast tracking without overshoot and oscillation. The corresponding turbine speed trajectories are shown in Fig. 7. It can be observed that the NN-based feedforward control N_{tf}^* captures the system transient dynamics very well and plays a dominant role which realizes a small feedback regulation in the outer-loop control.

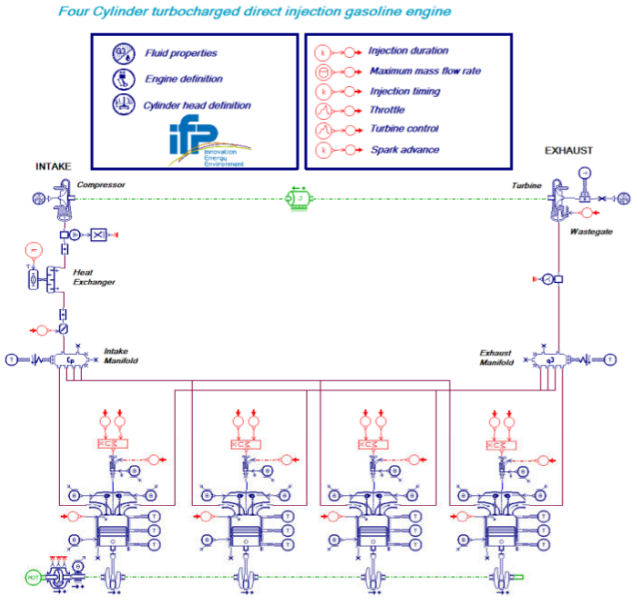

FIGURE 5. The higher fidelity model of the turbocharged gasoline engine in AMESim.

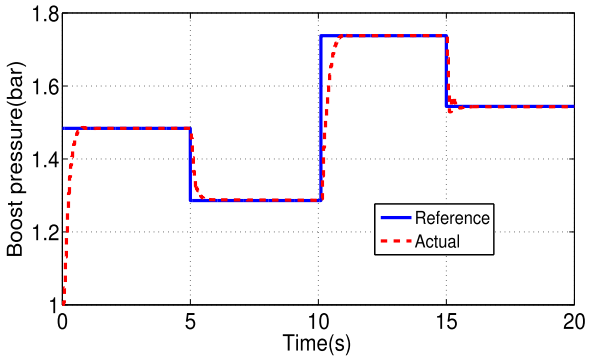

FIGURE 6. Simulation results on transient tracking performance evaluation at engine speed = 3000 rpm: Boost pressure trajectory.

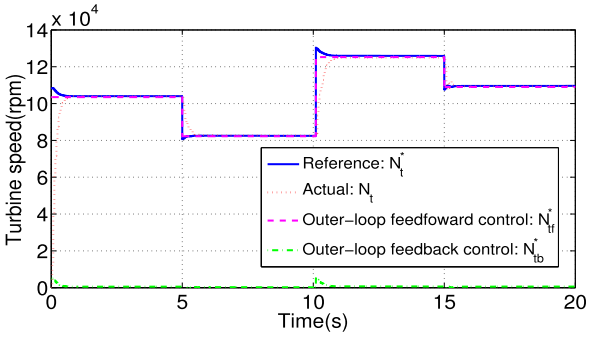

FIGURE 7. Simulation results on transient tracking performance evaluation at engine speed = 3000 rpm: Turbine speed trajectory.

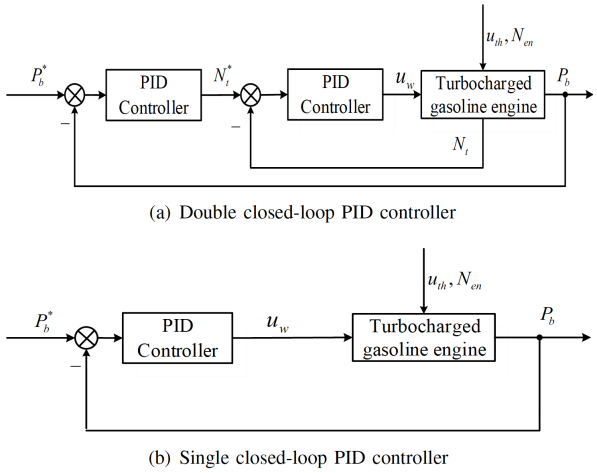

FIGURE 8. Structural diagram of the baseline PID controllers. (a) Double closed-loop PID controller. (b) Single closed-loop PID controller.

Overall, the proposed control system shows good transient tracking performance.

B. PERFORMANCE EVALUATION IN THE PRESENCE OF DISTURBANCES

In practice, as engine operating points vary, the control performance sensitivity with respect to the variation of engine speed should be tested. The proposed double closed-loop controller is tested and compared with two well-tuned baseline PID controllers: one is a double closed-loop PID controller referred to as DCL_PID in the context and the other is a single closed-loop PID controller referred to as SCL_PID in the context. The structural diagram of the two baseline PID controllers are shown in Fig. 8. Note that only one set of tuning parameters at the nominal engine speed (3000 rpm) is used for all the following tests. The tuning parameters of the baseline PID controllers are provided as follows.

(i) SCL_PID: $K_{P,SCL} = 250$, $K_{I,SCL} = 650$, $K_{D,SCL} = 0.1$;
(ii) DCL_PID outer-loop: $K_{P,DCL,O} = 0.4$, $K_{I,DCL,O} = 5.5$, $K_{D,DCL,O} = 0.001$;
(iii) DCL_PID inner-loop: $K_{P,DCL,I} = 0.007$, $K_{I,DCL,I} = 0.01$, $K_{D,DCL,I} = 0.00001$.

As shown in Fig. 9 and Fig. 10, at the nominal engine speed of 3000 *rpm*, all controllers are able to achieve fast tracking without overshoot and the control performances are similar. The comparison at engine speed of 2500 *rpm* is shown in Fig. 11 and Fig. 12. As shown in Fig. 11, the proposed double closed-loop nonlinear controller is still able to achieve good tracking performance, however, the two baseline PID controllers produce overshoot at transient.

Next, a worst case of a sudden operating change that the engine speed varies with a big step interval from 2500 *rpm* to 4000 *rpm* is considered and the associated results are shown in Fig. 13, Fig. 14 and Fig. 15. In this case, the boost pressure reference is set as $P_b^* = 1.4$ *bar*. In Fig. 14, the proposed

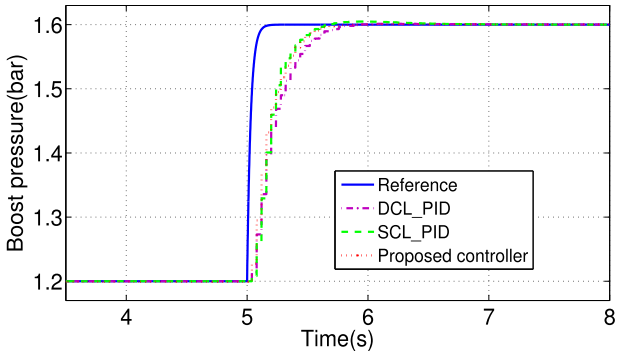

FIGURE 9. Performance comparison at engine speed = 3000 rpm: Boost pressure trajectory.

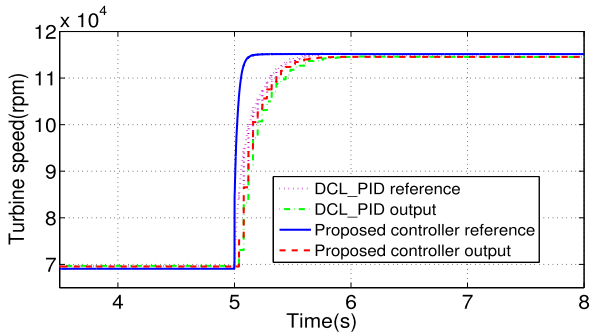

FIGURE 10. Performance comparison at engine speed = 3000 rpm: Turbine speed trajectory.

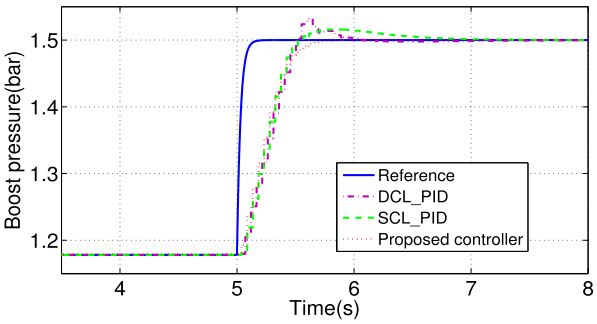

FIGURE 11. Performance comparison at engine speed = 2500 rpm: Boost pressure trajectory.

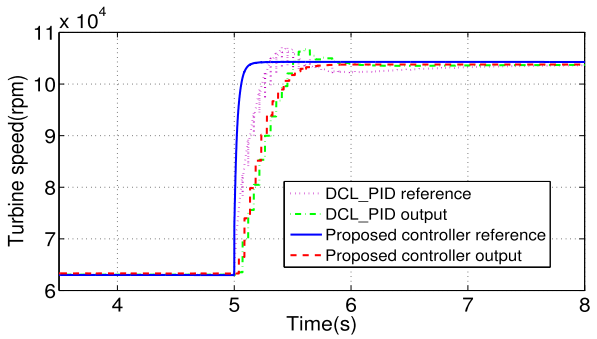

FIGURE 12. Performance comparison at engine speed = 2500 rpm: Turbine speed trajectory.

controller handles the transient with the smallest overshoot and shortest adjust time against the engine speed disturbance. In Fig. 15, the proposed controller generates a quicker turbine speed demand compared with DCL_PID to actively

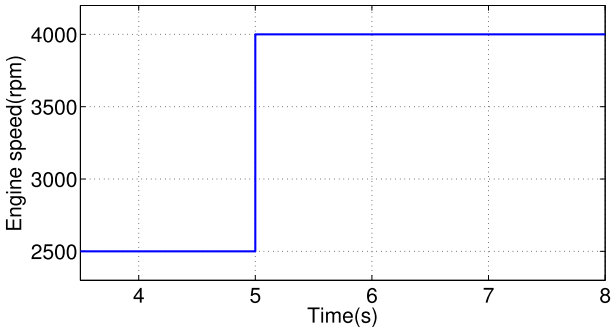

FIGURE 13. Performance comparison for the step change of engine speed from 2500 rpm to 4000 rpm: Engine speed trajectory.

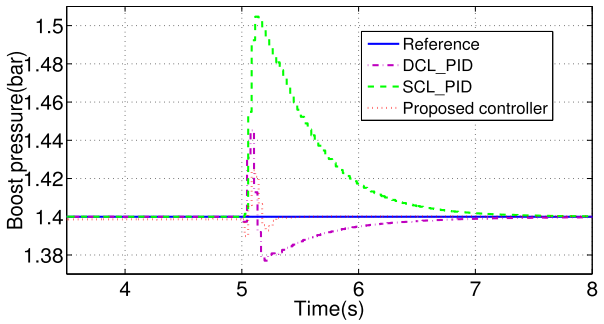

FIGURE 14. Performance comparison for the step change of engine speed from 2500 rpm to 4000 rpm: Boost pressure trajectory.

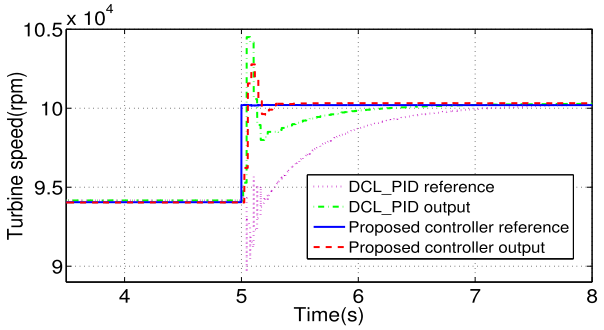

FIGURE 15. Performance comparison for the step change of engine speed from 2500 rpm to 4000 rpm: Turbine speed trajectory.

compensate the disturbance from the sudden change of the engine speed. Without a turbine speed planning in the outer loop, the SCL_PID fails to suppress the overshoot within the desired range. Since the performances of the proposed controller and DCL_PID are better than SCL_PID, it indicates the benefit and advantage of the application of applying the double closed-loop structure in turbocharged gasoline engine boost pressure control. Future work will focus on the experimental validation of the proposed controller.

V. CONCLUSION

This paper investigates the boost pressure tracking control of a turbo-charged gasoline engine. Taking the system nonlinearity and the long input-output regulation channel into account, a double closed-loop control scheme was proposed to achieve good transient tracking performance. To start with, a control-oriented mean value model of the turbocharged gasoline engine is developed. An outer loop feed-forward control was designed for achieving fast turbine speed tracking while a disturbance observer-based nonlinear inner loop control was designed for regulating the waste gate to compensate the nonlinearity and uncertainties. The stability and robustness of the whole closed-loop system was discussed. Simulation results demonstrated the proposed control system achieved good turbine speed and boost pressure tracking performance and had certain capability to reject disturbances due to operating variation.

REFERENCES

[1] P. Leduc, B. Dubar, A. Ranini, and G. Monnier, "Downsizing of gasoline engine: An efficient way to reduce CO_2 emissions," *Oil Gas Sci. Technol.*, vol. 58, no. 1, pp. 115–127, 2003.

[2] D. Petitjean, L. Bernardini, C. Middlemass, and S. M. Shahed, "Advanced gasoline engine turbocharging technology for fuel economy improvements," SAE Tech. Paper 2004-01-0988, 2004.

[3] L. Guzzella and C. Onder, *Introduction to Modeling and Control of Internal Combustion Engine Systems*. Heidelberg, Germany: Springer, 2009.

[4] N. Heintz, M. Mews, G. Stier, A. J. Beaumont, and A. D. Noble, "An approach to torque-based engine management systems," SAE Tech. Paper 2001-01-0269, 2001.

[5] G. Colin, Y. Chamaillard, G. Bloch, and A. Charlet, "Exact and linearized neural predictive control: A turbocharged si engine example," *J. Dyn. Syst. Meas., Control*, vol. 129, no. 4, pp. 527–533, 2007.

[6] S. Shinya, S. Nakagawa, H. Kakuya, T. Minowa, M. Nemoto, and H. Konno, "An accurate torque-based engine control by learning correlation between torque and throttle position," SAE Tech. Paper 2008-01-1015, 2008.

[7] D. He, Y. Shi, H. Li, and H. Du, "Multiobjective predictive cruise control for connected vehicle systems on urban conditions with InPA-SQP," *Optim. Control Appl. Methods*, vol. 40, no. 3, pp. 479–498, 2019.

[8] D. He, L. Wang, and J. Sun, "On stability of multiobjective NMPC with objective prioritization," *Automatica*, vol. 57, pp. 189–198, Jul. 2015.

[9] P. Wang, C. J. Zhu, and J. W. Gao, "Feedforward model predictive control of fuel-air ratio for lean-burn spark-ignition gasoline engines of passenger cars," *IEEE Access*, to be published. doi: 10.1109/ACCESS.2019.2919148.

[10] M. Santillo and A. Karnik, "Model predictive controller design for throttle and wastegate control of a turbocharged engine," in *Proc. Amer. Control Conf. (ACC)*, Jun. 2013, pp. 2183–2188.

[11] P. Ortner and L. del Re, "Predictive control of a diesel engine air path," *IEEE Trans. Control Syst. Technol.*, vol. 15, no. 3, pp. 449–456, May 2007.

[12] A. Bemporad, D. Bernardini, R. X. Long, and J. Verdejo, "Model predictive control of turbocharged gasoline engines for mass production," SAE Tech. Paper 2018-01-0875, 2018.

[13] Y. Hu, H. Chen, P. Wang, H. Chen, and L. Ren, "Nonlinear model predictive controller design based on learning model for turbocharged gasoline engine of passenger vehicle," *Mech. Syst. Signal Process.*, vol. 109, pp. 74–88, Sep. 2018.

[14] A. Y. Karnik, J. H. Buckland, and J. S. Freudenberg, "Electronic throttle and wastegate control for turbocharged gasoline engines," in *Proc. Amer. Control Conf. (ACC)*, Jun. 2005, pp. 4434–4439.

[15] P. Moulin, J. Chauvin, and B. Youssef, "Modelling and control of the air system of a turbocharged gasoline engine," *IFAC Proc. Volumes*, vol. 41, no. 2, pp. 8487–8494, 2008.

[16] Z. Qiu, M. Santillo, M. Jankovic, and J. Sun, "Composite adaptive internal model control and its application to boost pressure control of a turbocharged gasoline engine," *IEEE Trans. Control Syst. Technol.*, vol. 23, no. 6, pp. 2306–2315, Nov. 2015.

[17] A. Y. Karnik and M. Jankovic, "IMC based wastegate control using a first order model for turbocharged gasoline engine," in *Proc. Amer. Control Conf. (ACC)*, Jun. 2012, pp. 2872–2877.

[18] Z. Qiu, J. Sun, M. Jankovic, and M. Santillo, "Nonlinear internal model controller design for wastegate control of a turbocharged gasoline engine," *Control Eng. Pract.*, vol. 46, pp. 105–114, Jan. 2016.
[19] A. T. Nguyen, J. Lauber, and M. Dambrine, "Robust H_∞ control design for switching uncertain system: Appliation for turbocharged gasoline air system control," in *Proc. 51st IEEE Conf. Decis. Control (CDC)*, Dec. 2012, pp. 4265–4270.
[20] T. A. T. Nguyen, J. Lauber, and M. Dambrine, "Switching fuzzy control of the air system of a turbocharged gasoline engine," in *Proc. IEEE Int. Conf. Fuzzy Syst.*, Jun. 2012, pp. 1–7.
[21] X. Gong, K. Zaseck, I. Kolmanovsky, and H. Chen, "Dual-loop control of free piston engine generator," *IFAC-PapersOnLine*, vol. 48, no. 15, pp. 174–180, 2015.
[22] M. Feng and X. H. Jiao, "Double closed-loop control with adaptive strategy for automotive engine speed tracking system," *Int. J. Adapt. Control Signal Process.*, vol. 31, no. 1, pp. 1623–1635, 2017.
[23] P. Moulin and J. Chauvin, "Modeling and control of the air system of a turbocharged gasoline engine," *Control Eng. Pract.*, vol. 19, no. 3, pp. 287–297, Mar. 2011.
[24] J. H. Buckland, "Estimation methods for turbocharged spark ignition engines," Ph.D. dissertation, Dept. Elect. Eng., Syst., Univ. Michigan, Ann Arbor, MI, USA, 2009.
[25] L. Eriksson, "Modeling and control of turbocharged SI and DI engines," *Oil Gas Sci. Technol.*, vol. 62, no. 4, pp. 523–538, 2007.
[26] S. C. Sorenson, E. Hendricks, S. Magnusson, and A. Bertelsen, "Compact and accurate turbocharger modelling for engine control," *SAE Trans.*, vol. 114, pp. 1343–1353, Jan. 2005.
[27] M. Kao and J. J. Moskwa, "Turbocharged diesel engine modeling for nonlinear engine control and state estimation," *J. Dyn. Syst., Meas., Control*, vol. 117, no. 1, pp. 20–30, 1995.
[28] J. Melsa and J. J. Moskwa, *Linear Control Systems*. New York, NY, USA: McGraw-Hill, 1969.
[29] J. Tsinias, "Input to state stability properties of nonlinear systems and applications to bounded feedback stabilization using saturation," *ESAIM, Control, Optim. Calculus Variations*, vol. 2, pp. 57–87, Aug. 1997.
[30] M. R. Mokhtari, A. C. Braham, and B. Cherki, "Extended state observer based control for coaxial-rotor UAV," *ISA Trans.*, vol. 61, pp. 1–14, Mar. 2016.
[31] S. Xingling and W. Honglun, "Trajectory linearization control based output tracking method for nonlinear uncertain system using linear extended state observer," *Asian J. Control*, vol. 18, no. 1, pp. 316–327, 2016.
[32] Q. Zheng, L. Q. Gao, and Z. Gao, "On validation of extended state observer through analysis and experimentation," *J. Dyn. Syst., Meas., Control*, vol. 134, no. 2, 2012, Art. no. 024505.
[33] P. V. Kokotovic, "The joy of feedback: Nonlinear and adaptive," *IEEE Control Syst.*, vol. 12, no. 3, pp. 7–17, Jun. 1992.

XUN GONG received the B.S. degree in electrical engineering from Northeast Electrical Power University, in 2010, and the Ph.D. degree in control theory and control engineering from Jilin University, in 2016.

He was a Joint Ph.D. Student and a Postdoctoral Researcher with the University of Michigan, Ann Arbor, from 2013 to 2015 and from 2016 to 2018, respectively. He is currently an Assistant Professor with the AI School, Jilin University. His current research interests include model-based nonlinear control and optimal control, and control applications to automotive systems.

YAOHAN WANG received the B.S. degree in control theory and control engineering from Jilin University, Changchun, China, in 2019, where she is currently pursuing the M.S. degree with the Department of Control Science and Engineering. Her current research interest includes engine control.

HUAN CHEN received the B.S. degree in control theory and control engineering from Jilin University, Changchun, China, in 2016, where she is currently pursuing the M.S. degree with the Department of Control Science and Engineering. Her current research interests include nonlinear control and engine control.

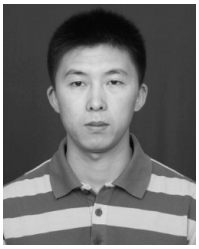

YUNFENG HU received the M.S. degree in basic mathematics and the Ph.D. degree in control theory and control engineering from Jilin University, Changchun, China, in 2008 and 2012, respectively, where he is currently an Associate Professor with the Department of Control Science and Engineering.

His current research interests include nonlinear control and automotive control.